

## Coupling of phonons and spin waves in a triangular antiferromagnet

Jung Hoon Kim<sup>1,\*</sup> and Jung Hoon Han<sup>1,2,\*</sup>

<sup>1</sup>*Department of Physics, BK21 Physics Research Division, Sungkyunkwan University, Suwon 440-746, Korea*

<sup>2</sup>*CSCMR, Seoul National University, Seoul 151-747, Korea*

(Received 26 April 2007; revised manuscript received 2 July 2007; published 17 August 2007)

We investigate the influence of the spin-phonon coupling in the triangular antiferromagnet where the coupling is of the exchange-striction type. The magnon dispersion is shown to be modified significantly at wave vector  $(2\pi, 0)$  and its symmetry-related points, exhibiting a rotonlike minimum and an eventual instability in the dispersion. Various correlation functions such as equal-time phonon correlation, spin-spin correlation, and local magnetization are calculated in the presence of the coupling.

DOI: [10.1103/PhysRevB.76.054431](https://doi.org/10.1103/PhysRevB.76.054431)

PACS number(s): 75.80.+q, 71.70.Ej, 77.80.-e

### I. INTRODUCTION

A number of recent experimental breakthroughs has revived interest in the phenomena of coupling between magnetic and electric (dipolar) degrees of freedom in a class of materials known as “multiferroics.”<sup>1</sup> Some noteworthy observations include the development of dipole moments accompanying the helical spin ordering,<sup>2,3</sup> displacement of magnetic ions at the onset of magnetic order in the triangular lattice  $\text{YMnO}_3$ ,<sup>4</sup> and adiabatic control of dipole moments through applied magnetic fields,<sup>5,6</sup> all of which unambiguously point to the strong coupling of electric and magnetic degrees of freedom. A number of theories has been advanced to establish a microscopic understanding of these couplings.<sup>7-13</sup>

The known mechanisms of the spin-polarization coupling fall into two categories. One is of the inverse Dzyaloshinskii-Moriya (DM) type, whereby the local dipole moment, denoted by  $u_{ij}$ , couples to the spins  $S_i$  by  $\sim u_{ij} \cdot \hat{e}_{ij} \times (S_i \times S_j)$ . Here, the unit vector  $\hat{e}_{ij}$  connects the centers of the magnetic ions at  $i$  and  $j$ . The microscopic origin of such coupling was investigated in, for instance, Refs. 7 and 11. The behavior of a large class of multiferroic materials can be understood on the basis of this coupling.<sup>1</sup> The other type arises from exchange striction, wherein the movement of the magnetic ions is assumed to directly influence the exchange integral and lead to the coupling  $\sim \hat{e}_{ij} \cdot (u_i - u_j) S_i \cdot S_j$ . The spin-lattice coupling in  $\text{RMn}_2\text{O}_5$  ( $R$ =rare earth) is believed to arise from this mechanism.<sup>14</sup>

More recently, the dynamical aspect of the magnetoelectric coupling has been investigated both experimentally<sup>15,16</sup> and theoretically.<sup>17</sup> The dynamical coupling is important because it can arise without the ordering of one or both of the degrees of freedom and can substantially influence the ac dielectric response<sup>15-17</sup> or even result in an exotic new phase with vector chirality.<sup>18</sup> The dynamics of the small fluctuations in the ordered phase of both the polarization and the spin was examined in Ref. 7 for the one-dimensional frustrated chain. A corresponding analysis of the coupled fluctuations has not yet been tried in the case of the exchange-striction mechanism or for other lattice geometries.

In the light of this, the triangular geometry offers a potentially fertile ground for the interplay of spin and dipolar degrees of freedom because of the tendency of spins to form a

spiral ( $120^\circ$ ) structure even without further frustrating interactions. The ground state is characterized by nonzero  $\langle S_i \cdot S_j \rangle$  as well as  $\langle S_i \times S_j \rangle$ , which may result in spin-dipole interactions of both DM and exchange striction types. Furthermore, quite recently, it was shown that a spin  $S=5/2$  triangular antiferromagnet in  $\text{RbFe}(\text{MoO}_4)_2$  (Ref. 19) develops spontaneous polarization along the  $c$  axis as the spins order in the  $ab$  plane. This and another triangular lattice compound,  $\text{YMnO}_3$ , offer promising examples, where the interplay of spin and dipolar degrees of freedom can be revealed in detail. In particular, the dynamical aspect of the spin-dipole coupling in the triangular lattice remains largely unexplored and a theoretical consideration of their interplay would be timely.

In this paper, we examine the coupled dynamics of Heisenberg spins and the local dipolar variable (hereafter referred to simply as phonons) on the triangular lattice, assuming the exchange-striction interaction. In Sec. II, the model Hamiltonian is introduced and solved within the Holstein-Primakoff theory. A number of physical quantities, such as the local magnetic moment, phonon correlation function, and the dynamic spin-spin correlation, are derived in Sec. III. Conclusions and the relevance of our work to existing experiments can be found in Sec. IV.

### II. SPIN-PHONON MODEL

The spin-phonon coupled Hamiltonian in the exchange-striction picture reads<sup>20</sup>

$$H = \sum_{\langle ij \rangle} [J_0 - J_1 \hat{e}_{ji} \cdot (u_j - u_i)] S_i \cdot S_j + \sum_i \left( \frac{p_i^2}{2m} + \frac{K}{2} u_i^2 \right), \quad (1)$$

where the antiferromagnetic exchange integral  $J_{ij}$  connecting the two nearest-neighbor Heisenberg spins is expanded to first order in the displacement  $u_i$  of each atomic site  $i$ .  $\hat{e}_{ji}$  is the unit vector extending from  $i$  to  $j$  atomic sites. The terms proportional to  $J_1$  define the spin-phonon coupling. The Heisenberg spin of magnitude  $S$  is represented by  $S_i$ , and the two-dimensional displacement vectors and their canonical conjugate operators by  $u_i$  and  $p_i$ . We separate the Hamiltonian into two parts,  $H = H_0 + H_1$ , where  $H_1$  is the spin-

phonon interaction term and  $H_0$  consists of the Heisenberg and phonon Hamiltonians,

$$H_0 = J_0 \sum_{\langle ij \rangle} S_i \cdot S_j + \sum_i \left( \frac{p_i^2}{2m} + \frac{K}{2} u_i^2 \right),$$

$$H_1 = J_1 \sum_{\langle ij \rangle} \hat{e}_{ji} \cdot (u_i - u_j) S_i \cdot S_j. \quad (2)$$

The classical ground state of the above Hamiltonian was worked out in Ref. 20. It was shown that, despite the spin-phonon coupling term, the classical spin configuration is that of the pure Heisenberg model on the triangular lattice with the neighboring spins at a  $120^\circ$  angle with each other.

Although the spin-phonon interaction does not produce any observable effect in the ground state spin configuration, the excitation spectra of the lattice (phonons) and the spins (magnons) will be mixed due to  $H_1$ .

The small fluctuations near the ground state can be analyzed within the standard Holstein-Primakoff approach after first rotating the spin operators according to their classical spin orientations defined by  $\langle S_i \rangle = (0, \sin \phi_i, \cos \phi_i)$ , where  $\phi_i$  is the angle the spin makes with the  $z$  axis at site  $i$ . All the spins are assumed to lie in the  $yz$  plane, which also coincides with the plane of the lattice itself. After performing the Bogoliubov rotation defined by the angle  $\tanh \phi_k = 3\gamma_k / (2 + \gamma_k)$  to obtain the spin wave spectrum, the Hamiltonian  $H_0$  reads

$$H_0 = \sum_k \varepsilon_k \alpha_k^\dagger \alpha_k + \omega_0 \sum_k (b_{ky}^\dagger b_{ky} + b_{kz}^\dagger b_{kz}), \quad (3)$$

with the spin wave dispersion

$$\varepsilon_k = \frac{3J_0 S}{2} \sqrt{(1 - \gamma_k)(1 + 2\gamma_k)}. \quad (4)$$

Here,  $\gamma_k = (1/3) \sum_{\alpha=1}^3 \cos[k \cdot \hat{e}_\alpha]$  with  $\hat{e}_1 = (1, 0)$ ,  $\hat{e}_2 = (-1/2, \sqrt{3}/2)$ , and  $\hat{e}_3 = (-1/2, -\sqrt{3}/2)$  in the basis spanned by  $z$  and  $-y$  vectors. The lattice constant is taken to unity. Phonon operators in the  $y$  and  $z$  directions are also introduced above as  $b_{ky}$  and  $b_{kz}$  as well as the phonon energy  $\omega_0$ .

The spin-phonon Hamiltonian  $H_1$  can be expanded to second order in the magnon and phonon operators. The full spin-phonon Hamiltonian to quadratic order is given in the simple form ( $\bar{k} \equiv -k$ ) (Ref. 21)

$$H = \sum_k [\varepsilon_k \alpha_k^\dagger \alpha_k + \omega_0 \beta_k^\dagger \beta_k + i\lambda_k (\alpha_k^\dagger - \alpha_{\bar{k}}) (\beta_k + \beta_{\bar{k}}^\dagger)], \quad (5)$$

where

$$\lambda_k = -\frac{3}{4} J_1 S \sqrt{\frac{S}{m\omega_0}} e^{\phi_k/2} \sqrt{\chi_{ky}^2 + \chi_{kz}^2},$$

$$\chi_{ky} = \cos(k \cdot \hat{e}_3) - \cos(k \cdot \hat{e}_2),$$

$$\sqrt{3}\chi_{kz} = 2 \cos(k \cdot \hat{e}_1) - \cos(k \cdot \hat{e}_2) - \cos(k \cdot \hat{e}_3). \quad (6)$$

Note that only the following linear combination of the phonons participates in the interaction with the magnons:

$$\beta_k = \frac{\chi_{ky} b_{ky} + \chi_{kz} b_{kz}}{\sqrt{\chi_{ky}^2 + \chi_{kz}^2}}. \quad (7)$$

The rotation of the Hamiltonian to the diagonalized basis is affected by a series of canonical transformations given by  $\psi_k = W_k X_k Y_k \Psi_k$ , where  $\Psi_k$ , the diagonal operators, are given by  $(\mathcal{A}_{1k}, \mathcal{A}_{2k}, \mathcal{A}_{1\bar{k}}^\dagger)^T$ . The respective matrices are defined as follows:

$$W_k = \begin{pmatrix} \cos \frac{\theta_k}{2} & 0 & -i \sin \frac{\theta_k}{2} & 0 \\ 0 & i \sin \frac{\theta_k}{2} & 0 & \cos \frac{\theta_k}{2} \\ -i \sin \frac{\theta_k}{2} & 0 & \cos \frac{\theta_k}{2} & 0 \\ 0 & \cos \frac{\theta_k}{2} & 0 & i \sin \frac{\theta_k}{2} \end{pmatrix}, \quad \begin{cases} \sin \theta_k = 2\lambda_k / \sqrt{(\varepsilon_k - \omega)^2 + 4\lambda_k^2} \\ \cos \theta_k = (\varepsilon_k - \omega) / \sqrt{(\varepsilon_k - \omega)^2 + 4\lambda_k^2} \end{cases}$$

$$X_k = \begin{pmatrix} \cosh \frac{\nu_k}{2} & -i \sinh \frac{\nu_k}{2} & 0 & 0 \\ i \sinh \frac{\nu_k}{2} & \cosh \frac{\nu_k}{2} & 0 & 0 \\ 0 & 0 & \cosh \frac{\nu_k}{2} & -i \sinh \frac{\nu_k}{2} \\ 0 & 0 & i \sinh \frac{\nu_k}{2} & \cosh \frac{\nu_k}{2} \end{pmatrix}, \quad \begin{cases} \sinh \nu_k = \Delta_k / \sqrt{\Delta_k^2 - \Lambda_k^2} \\ \cosh \nu_k = \Lambda_k / \sqrt{\Delta_k^2 - \Lambda_k^2} \end{cases}$$

$$Y_k = \begin{pmatrix} \cosh \frac{\mu_{1k}}{2} & 0 & 0 & \sinh \frac{\mu_{1k}}{2} \\ 0 & \cosh \frac{\mu_{2k}}{2} & \sinh \frac{\mu_{2k}}{2} & 0 \\ 0 & \sinh \frac{\mu_{2k}}{2} & \cosh \frac{\mu_{2k}}{2} & 0 \\ \sinh \frac{\mu_{1k}}{2} & 0 & 0 & \cosh \frac{\mu_{1k}}{2} \end{pmatrix}, \quad \begin{cases} \sinh \mu_{1k} = \Gamma_k/E_{1k}, & \sinh \mu_{2k} = \Gamma_k/E_{2k}, \\ \cosh \mu_{1k} = \mathcal{E}_{1k}/E_{1k}, & \cosh \mu_{2k} = \mathcal{E}_{2k}/E_{2k}, \end{cases} \quad (8)$$

where  $\Lambda_k = \lambda_k \cos \theta_k$ ,  $\Gamma_k = \lambda_k \sin \theta_k$ ,  $\Delta_k = \frac{\Delta_{1k} + \Delta_{2k}}{2}$ ,  $\delta_k = \frac{\Delta_{1k} - \Delta_{2k}}{2}$ ,  $\mathcal{E}_{1k,2k} = \sqrt{\Delta_k^2 - \Lambda_k^2 \pm \delta_k}$ ,  $E_{1k,2k} = \sqrt{\mathcal{E}_{1k,2k}^2 - \Gamma_k^2}$ , and  $\Delta_{1k,2k} = \frac{\varepsilon_k + \omega}{2} \pm \frac{1}{2} \sqrt{(\varepsilon_k - \omega)^2 + 4\lambda_k^2}$ . The final form of the Hamiltonian is

$$Y_k^\dagger X_k^\dagger W_k^\dagger \mathcal{H}_k W_k X_k Y_k = \text{diag}(E_{1k}, E_{2k}, E_{2k}, E_{1k}),$$

$$H = \sum_k (E_{1k} A_{1k}^\dagger A_{1k} + E_{2k} A_{2k}^\dagger A_{2k}). \quad (9)$$

The sum  $\sum_k$  is over the entire Brillouin zone. For any given  $k$ , we have  $E_{1k} \geq E_{2k}$ , constituting an upper and lower branch of the spectra.

A plot of  $E_{1k}$  and  $E_{2k}$  in Fig. 1 shows the change in the magnon and the phonon spectrum as  $J_1$  is increased. The most notable feature in the coupled energy spectrum is the appearance of the rotonlike minimum at a set of  $k$  points in the Brillouin zone. When  $J_1$  equals the threshold value, e.g.,  $J_{1c} \equiv 0.321$  for  $S=1/2$ ,  $\omega_0=0.5$ , and the phonon wave function width  $m\omega_0=1$ ,  $E_{2k}$  touches zero at  $k=(2\pi, 0)$ ,  $(0, 2\pi/\sqrt{3})$ , and all their sixfold symmetry-related points indicated as white dots in Fig. 1(c). The original zeros of the magnon spectrum at  $\pm(4\pi/3, 0)$  remain intact through non-zero  $J_1$ .

As this happens, one has a new spin-ordered pattern illustrated in Fig. 2 becoming degenerate with the original  $120^\circ$  ordered phase. This new pattern is obtained by rotating spins counterclockwise by  $120^\circ$  along the  $\hat{e}_1$  direction and clockwise by  $60^\circ$  along the  $\hat{e}_2$  direction. The state where the spins are rotated in the opposite directions will also be degenerate, carrying the opposite sense of chirality. In terms of ordering wave vectors, the new ground states are characterized by  $Q' = \pm(2\pi/3, 0)$  instead of  $Q = \pm(4\pi/3, 0)$  as in the  $120^\circ$  ordered phase.

### III. PHYSICAL QUANTITIES

The local staggered magnetization (uniform magnetization in the rotated basis),  $\langle \mathbf{S} \rangle \equiv (1/N) \sum_i \langle \mathbf{S}_i^z \rangle$ , is modified due to the spin-phonon coupling. The quantum correction, defined as the difference of the classical and quantum averages  $S - \langle \mathbf{S} \rangle$ , reads

$$\sum_k \left( \sinh^2 \frac{\phi_k}{2} + \cosh \phi_k \langle \alpha_k^\dagger \alpha_k \rangle - \sinh \phi_k \langle \alpha_k^\dagger \alpha_k^- \rangle \right), \quad (10)$$

which is plotted at  $T=0$  in Fig. 3 for various spin values as the coupling strength is varied. In small powers of  $\lambda_k$ , one obtains the following perturbative expression as the quantum correction:

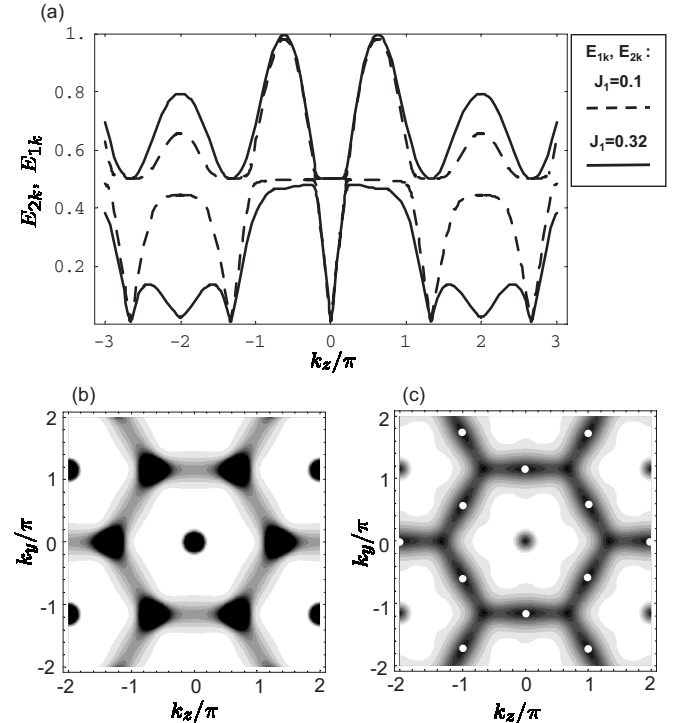


FIG. 1. (a) Dispersion along the  $(k_z, 0)$  direction for  $E_{1k}$  and  $E_{2k}$  for two choices of spin-phonon coupling,  $J_1=0.1$  (dashed) and  $J_1=0.32$  (solid). We have chosen  $J_0=3.7$  to normalize the maximum energy value to 1. Other parameters are  $S=1/2$ ,  $\omega_0=0.5$ , and  $m=2$ . The phonon wave function width is chosen  $1/\sqrt{m\omega_0}=1$ , equal to the lattice constant. The level repulsion is particularly severe at  $(k_x, k_y)=(2\pi, 0)$  as the strength of the coupling is increased. [(b) and (c)] Contour plots of the low-energy branch  $E_{2k}$  for (b)  $J_1=0.1$  and (c) 0.32. Indicated as white dots in (c) are the  $k$  points, where  $E_{2k}$  reaches zero at the critical spin-phonon coupling.

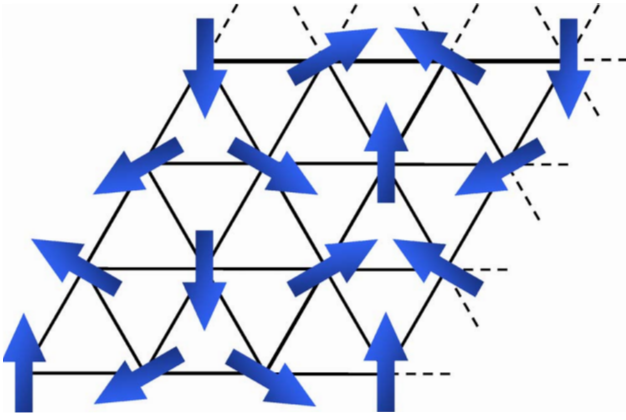


FIG. 2. (Color online) The new emergent spin configuration for the critical spin-phonon coupling value  $J_1 = J_{1c}$  corresponding to the ordering wave vector  $Q' = (4\pi/3 \pm 2\pi, 0)$  or, equivalently,  $Q' = \pm(2\pi/3, 0)$ . This configuration becomes degenerate with those at  $Q = \pm(4\pi/3, 0)$  when  $J_1$  equals  $J_{1c}$ .

$$\sum_k \sinh^2 \frac{\phi_k}{2} + \sum_k \frac{\lambda_k^2 \cosh \phi_k}{(\varepsilon_k + \omega_0)^2} + \sum_k \frac{\lambda_k^2 \sinh \phi_k}{\varepsilon_k(\varepsilon_k + \omega_0)}. \quad (11)$$

The first term is the usual quantum fluctuation correction, and the latter two account for further corrections due to spin-phonon coupling. There is only a tiny change in the local magnetization affected by the spin-phonon coupling. On the other hand, the upturn found in Fig. 3 as  $J_1$  is driven up to its critical value is probably indicative of the diverging quantum correction as the new ground state is approached. Due to the finite phonon mass  $\omega_0$ , the spin-phonon coupling effects are not apparent until very near the criticality.

The equal-time phonon correlation function  $\langle \mathbf{u}_i \cdot \mathbf{u}_j \rangle$ , which will be short ranged  $\langle \mathbf{u}_i \cdot \mathbf{u}_j \rangle_0 = \delta_{ij}$  (since we have chosen  $m\omega_0 = 1$ ) in the absence of spin-phonon coupling, now reads

$$\langle \mathbf{u}_i \cdot \mathbf{u}_j \rangle - \langle \mathbf{u}_i \cdot \mathbf{u}_j \rangle_0 = \frac{\sqrt{3}}{16\pi^2} \int_{\text{BZ}} e^{ik \cdot (r_i - r_j)} (G_k - 1) d^2k,$$

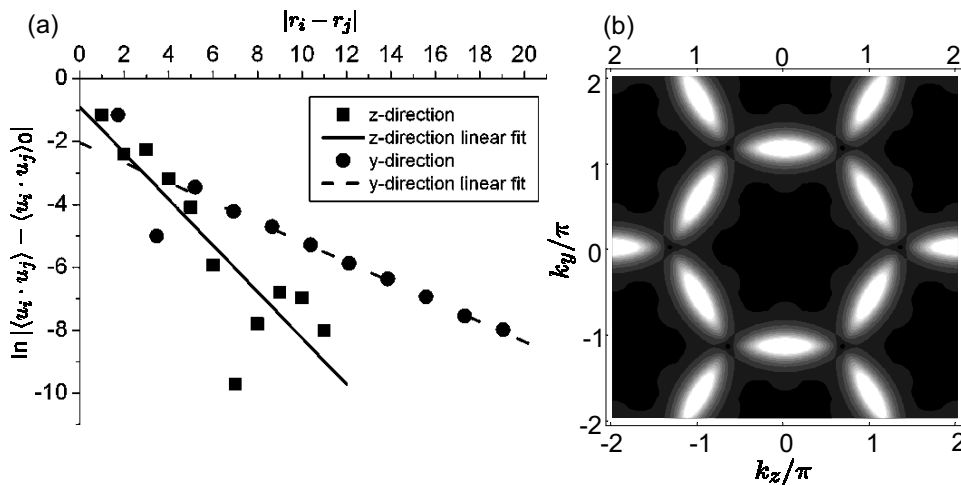


FIG. 4. (a) Logarithmic plots of the correlation function  $|\langle \mathbf{u}_i \cdot \mathbf{u}_j \rangle - \langle \mathbf{u}_i \cdot \mathbf{u}_j \rangle_0|$  in the  $z$  (solid) and  $y$  (dashed) directions. Using the same parameter values as in Fig. 1, the correlation length can be extracted as  $\sim 1.36$  and  $\sim 3.16$  lattice constants in the  $z$  and  $y$  directions, respectively. (b) Plot of  $G_k - 1$ . Bright regions indicate peaks in  $G_k - 1$ .

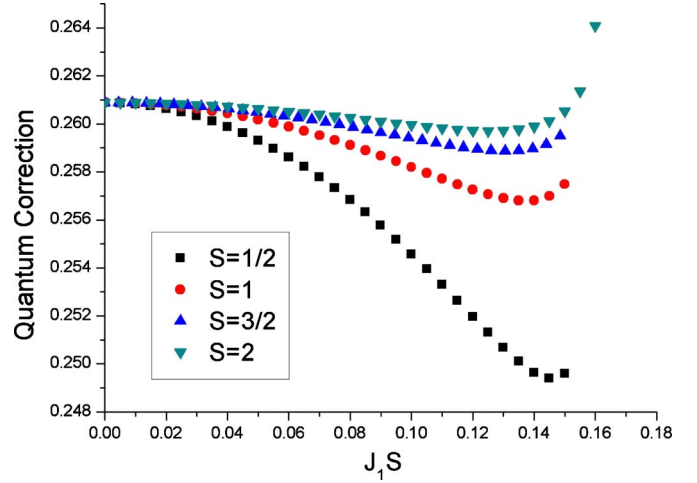


FIG. 3. (Color online) Plot of the quantum correction versus the coupling strength for various spin values and  $0 < J_1 S < J_{1c} S$ . The critical coupling strength depends on  $S$ , while the product  $J_1 S$  is nearly independent of  $S$ . Choices of other parameters are the same as in Fig. 1.

$$G_k = \langle (\beta_k + \beta_k^\dagger)(\beta_k^\dagger + \beta_k) \rangle, \quad (12)$$

at zero temperature. A logarithmic plot of  $|\langle \mathbf{u}_i \cdot \mathbf{u}_j \rangle - \langle \mathbf{u}_i \cdot \mathbf{u}_j \rangle_0|$  is given in Fig. 4, showing an exponential decay with a correlation length which depends on the parameters. The momentum space correlation  $G_k$  shows pronounced peaks around  $k = (0, 2\pi/\sqrt{3})$  and other symmetry-related points, as shown in Fig. 4(b). These are the same points where  $E_{2k}$  shows pronounced minima for large  $J_1$ . Detection of such peaks in the phonon structure factor  $G_k$  will be instrumental in identifying the spin-phonon coupling in a triangular anti-ferromagnet.

The spin-spin correlation function  $\langle S_j^+(t) S_i^-(0) \rangle$  can be an effective probe of the spin-phonon coupling. Using the straightforward algebra, we have calculated the absorption spectra  $I(k, \omega)$  as the imaginary part of the Fourier transform of the spin-spin correlation function,

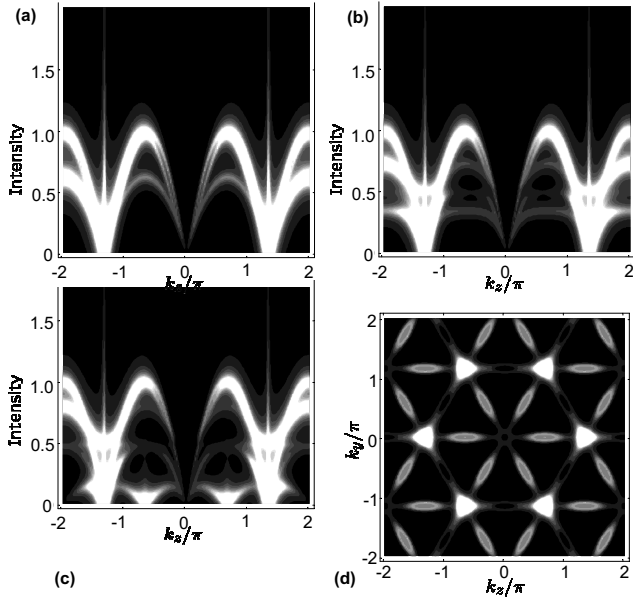


FIG. 5. Plots of the spectral function  $I(k, \omega)$  along the  $k_z$  direction ( $k_y=0$ ) for (a)  $J_1=0$ , (b)  $J_1=0.2$ , and (c)  $J_1=0.32$ . Emergence of a new low-energy feature at  $k_z=2\pi/3$  for  $J_1$  close to the critical value  $J_{1c}=0.321$  is apparent in (c). (d) Plot of  $I(k_z, k_y, \omega=0.1)$  clearly indicates new intensity peaks at  $(2\pi/3, 0)$  and other symmetry points (elongated and shaded), while the bright patterns at  $(4\pi/3, 0)$ , etc., are due to the original spin waves.

$$I(k, \omega) = \frac{\pi S}{8} \left\{ \sum_{\alpha=1,2} e^{\phi_{k_\alpha}} [(B_{1k_\alpha} - A_{1k_\alpha}) \delta(\omega - E_{1k_\alpha}) + (B_{2k_\alpha} - A_{2k_\alpha}) \delta(\omega - E_{2k_\alpha})] + 2e^{-\phi_k} [(A_{1k} + B_{1k}) \times \delta(\omega - E_{1k}) + (A_{2k} + B_{2k}) \delta(\omega - E_{2k})] \right\}, \quad (13)$$

which is plotted in Fig. 5. The functions appearing in Eq. (22) are defined as  $k_{1,2}=k \pm (4\pi/3, 0)$  and

$$\begin{aligned} A_{1k} &= \sinh \mu_{1k} (\cos \theta_k + \cosh \nu_k) - \cosh \mu_{1k} \sin \theta_k \sinh \nu_k, \\ A_{2k} &= \sinh \mu_{2k} (\cos \theta_k - \cosh \nu_k) - \cosh \mu_{2k} \sin \theta_k \sinh \nu_k, \\ B_{1k} &= \cosh \mu_{1k} (\cos \theta_k + \cosh \nu_k) - \sinh \mu_{1k} \sin \theta_k \sinh \nu_k, \\ B_{2k} &= \cosh \mu_{2k} (\cosh \nu_k - \cos \theta_k) + \sinh \mu_{2k} \sin \theta_k \sinh \nu_k. \end{aligned} \quad (14)$$

The flattening and the eventual collapse of the excitation band found earlier now manifests itself as intensity patterns

at  $(k_z, k_y) = (2\pi/3, 0)$  and its rotational counterparts, as can be seen in Fig. 5(d).

#### IV. DISCUSSION

In summary, we have considered the magnon-phonon coupling in the exchange-striction coupled triangular lattice antiferromagnet for Heisenberg spins in the Holstein-Primakoff approach. The dynamics of the lattice and the spins is coupled to produce interesting modifications in the excitation spectra, in particular, (i) the significant lowering of the magnon excitation energy at wave vector transfer  $\pm 2\pi$ , as indicated in Fig. 1 and (ii) the concordant variation in the phonon structure factor, as shown in Fig. 4(b). Detection of an additional low-energy spectra in the spin spectral function  $I(k, \omega)$  and in the phonon structure factor  $G_k$  through neutron scattering experiments will be a clear hint of the strong spin-phonon coupling.

Naively speaking, integrating out the phonon coordinate from Eq. (1) would generate the effective interaction,  $\sim -\sum_i (\sum_{j=NN} i \hat{e}_{ij} S_i \cdot S_j)^2$ , which embodies the ferromagnetic biquadratic exchange,  $-(S_i \cdot S_j)^2$ , and some three-body interactions as well. A quantum spin model involving quadratic and biquadratic exchanges was considered extensively<sup>22</sup> following the discovery of the liquidlike ground state in the triangular antiferromagnet  $\text{NiGa}_2\text{S}_4$ .<sup>23</sup> The ground state revealed correlations, dynamic on the scale of  $\sim 1$  ns, of a period-six spin orientation ( $60^\circ$  angles between nearest neighbors), quite unlike the period-three orientation ( $120^\circ$  angles between nearest neighbors) expected in the triangular lattice. It is not easy to reproduce such a spin structure in the mean field solution of the spin models considered in Ref. 22. In fact, the spin-spin correlation observed in  $\text{NiGa}_2\text{S}_4$  is almost exactly the one shown in Fig. 2. To correctly account for the observed periodicity of spins in  $\text{NiGa}_2\text{S}_4$ , one would have to consider an extended-neighbor interaction as in Ref. 24 or some dynamical consequence of spin-phonon coupling as in the present paper.

#### ACKNOWLEDGMENTS

We wish to acknowledge fruitful discussions with Chenglong Jia. Discussions with Satoru Nakatsuji on  $\text{NiGa}_2\text{S}_4$  are also gratefully acknowledged. J. H. H. was partly supported by the Samsung Research Fund, Sungkyunkwan University, 2006.

\*hanjh@skku.edu

<sup>1</sup>A recent review of the subject can be found in Y. Tokura, *Science* **312**, 1481 (2006); S.-W. Cheong and M. Mostovoy, *Nat. Mater.* **6**, 13 (2007).

<sup>2</sup>G. Lawes *et al.*, *Phys. Rev. Lett.* **95**, 087205 (2005).

<sup>3</sup>M. Kenzelmann, A. B. Harris, S. Jonas, C. Broholm, J. Schefer, S. B. Kim, C. L. Zhang, S. W. Cheong, O. P. Vajk, and J. W. Lynn, *Phys. Rev. Lett.* **95**, 087206 (2005).

- <sup>4</sup>S. Lee, A. Pirogov, J. H. Han, J. G. Park, A. Hoshikawa, and T. Kamiyama, *Phys. Rev. B* **71**, 180413(R) (2005).
- <sup>5</sup>T. Kimura, T. Goto, H. Shintani, K. Ishizaka, T. Arima, and Y. Tokura, *Nature (London)* **426**, 55 (2003).
- <sup>6</sup>N. Hur, S. Park, P. A. Sharma, J. S. Ahn, S. Guha, and S.-W. Cheong, *Nature (London)* **429**, 392 (2004).
- <sup>7</sup>H. Katsura, N. Nagaosa, and A. V. Balatsky, *Phys. Rev. Lett.* **95**, 057205 (2006).
- <sup>8</sup>M. Mostovoy, *Phys. Rev. Lett.* **96**, 067601 (2006).
- <sup>9</sup>I. A. Sergienko and E. Dagotto, *Phys. Rev. B* **73**, 094434 (2006).
- <sup>10</sup>A. B. Harris, T. Yildirim, A. Aharony, and O. Entin-Wohlman, *Phys. Rev. B* **73**, 184433 (2006).
- <sup>11</sup>C. Jia, S. Onoda, N. Nagaosa, and J. H. Han, *Phys. Rev. B* **74**, 224444 (2006); arXiv:cond-mat/0701614.
- <sup>12</sup>B. B. van Aken, T. T. M. Palstra, A. Filippetti, and N. A. Spaldin, *Nat. Mater.* **3**, 164 (2004).
- <sup>13</sup>C. Jia and J. H. Han, *Phys. Rev. B* **73**, 172411 (2006).
- <sup>14</sup>L. C. Chapon, G. R. Blake, M. J. Gutmann, S. Park, N. Hur, P. G. Radaelli, and S. W. Cheong, *Phys. Rev. Lett.* **93**, 177402 (2004); L. C. Chapon, P. G. Radaelli, G. R. Blake, S. Park, and S. W. Cheong, *ibid.* **96**, 097601 (2006).
- <sup>15</sup>A. Pimenov *et al.*, *Nat. Phys.* **2**, 97 (2006).
- <sup>16</sup>A. B. Sushkov, R. V. Aguilar, S. Park, S. W. Cheong, and H. D. Drew, *Phys. Rev. Lett.* **98**, 027202 (2007).
- <sup>17</sup>H. Katsura, A. V. Balatsky, and N. Nagaosa, *Phys. Rev. Lett.* **98**, 027203 (2007).
- <sup>18</sup>S. Onoda and N. Nagaosa, *Phys. Rev. Lett.* (to be published).
- <sup>19</sup>M. Kenzelman *et al.*, arXiv:cond-mat/0701426.
- <sup>20</sup>C. Jia, J. H. Nam, J. S. Kim, and J. H. Han, *Phys. Rev. B* **71**, 212406 (2005).
- <sup>21</sup>In the unrotated spin basis, the phonon at momentum  $k$  couples to the magnon at  $k \pm Q$ , where  $Q$  is the ordering wave vector  $(4\pi/3, 0)$ . Due to the rotation that aligns the spins ferromagnetically, the magnon-phonon coupling appears between the same  $k$  states.
- <sup>22</sup>H. Tsunetsugu and M. Arikawa, *J. Phys. Soc. Jpn.* **75**, 083701 (2006); A. Läuchli, F. Mila, and K. Penc, *Phys. Rev. Lett.* **97**, 087205 (2006); S. Bhattacharjee, V. B. Shenoy, and T. Senthil, *Phys. Rev. B* **74**, 092406 (2006).
- <sup>23</sup>S. Nakatsuji *et al.*, *Science* **309**, 1697 (2005).
- <sup>24</sup>K. Takubo *et al.*, *Phys. Rev. Lett.* (to be published).